Title

Single particle ICP-MS and GC-MS provide a new insight into the formation mechanisms during the green synthesis of AgNPs

Journal

New Journal of Chemistry, 43(9)

ISSN

1144-0546

Authors

Zhang, Huiling
Huang, Yuxiong
Gu, Jianqiang
et al.

Publication Date

2019-02-25

DOI

10.1039/c8nj06291a

Peer reviewed

NJC

PAPER

View Article Online
View Journal | View Issue

Cite this: *New J. Chem.*, 2019, **43**, 3946

Single particle ICP-MS and GC-MS provide a new insight into the formation mechanisms during the green synthesis of AgNPs†

Huiling Zhang, ‡[a] Yuxiong Huang, ‡[bc] Jianqiang Gu,[a] Arturo Keller,[b] Yuwei Qin,[b] Yue Bian,[d] Kun Tang,[d] Xiaolei Qu,[a] Rong Ji*[a] and Lijuan Zhao*[a]

Green synthesis of metallic nanoparticles (NPs) using plant extracts has received considerable attention due to its environmentally and economically friendly nature. Various metabolites in plants such as amino acids, organic acids, sugars and phenolic compounds have been speculated to be responsible for the synthesis of metallic NPs in previous studies. However, to date, there has been a lack of direct evidence linking specific metabolites to the reduction of metal ions to form metallic NPs. Here, AgNPs are synthesized using cucumber leaf extract and characterized by UV-visible spectroscopy, dynamic light scattering (DLS) and transmission electron spectroscopy (TEM). Single particle inductively coupled plasma mass spectrometry (sp-ICP-MS) was used to investigate the size of newly synthesized NPs as well as the kinetics of particle formation. Gas chromatography–mass spectrometry (GC-MS) based metabolomics identified and quantified 245 metabolites in cucumber leaf extracts. By comparing the concentrations of metabolites before and after the reaction, the metabolites responsible for the synthesis were screened out. Reducing sugars (cellobiose, ribulose-5-phosphate, melibiose, 2-deoxy-D-glucose, tagatose, fructose, ribose, 3,6-anhydro-D-galactose) were markedly decreased after the reaction, indicating that reducing sugars are involved in the biosynthesis process and possibly function as reducing agents. The key thermodynamic data of the reaction between Ag^+ and reducing sugars were obtained by using isothermal titration calorimetry (ITC), which further confirmed the interaction between Ag^+ and metabolites. This study provides a deep insight into the reaction process and mechanism of green synthesized AgNPs.

Received 15th December 2018,
Accepted 25th January 2019

DOI: 10.1039/c8nj06291a

rsc.li/njc

Introduction

Green synthesis of nanoparticles (NPs) has become a promising field of research in recent years. Plant-mediated biosynthesis of metallic nanoparticles is comparatively cost-effective and environmentally-friendly compared to chemical methods.[1] There are many studies employing different plant extracts to mediate the biosynthesis of various metal or metal oxide NPs.[2–12] However, current knowledge of key metabolites involved in the biosynthesis and the mechanisms of nanoparticle formation is quite poor.[13] Understanding the actual mechanisms underlying nanoparticle formation is necessary to develop a rational approach to control the size, shape and crystallinity of the NPs.[13]

Plants generate a large number of primary metabolites such as organic acids, sugars, and amino acids; as well as numerous secondary metabolites which play an important role in the defense mechanism and act as antioxidants, such as phenolic compounds, ascorbic acid, quinones, flavonoids, terpenoids and polysaccharides. Among them, reducing sugars, proteins and polyphenols have been postulated to act as reducing and stabilizing agents for synthesis of metal and metal oxide NPs in previous reports.[3,14–16] Beattie and Haverkamp[17] found that chloroplasts, a subcellular organelle that produces abundant amounts of reducing sugars (*i.e.* glucose and fructose), accumulated the highest amount of silver nanoparticles (AgNPs) and thus

[a] *State Key Laboratory of Pollution Control and Resource Reuse, School of Environment, Nanjing University, Nanjing 210023, China. E-mail: ji@nju.edu.cn, ljzhao@nju.edu.cn; Fax: +86 025-8968 0581; Tel: +86 025-8968 0581*
[b] *Bren School of Environmental Science & Management, University of California, Santa Barbara, California 93106-5131, USA*
[c] *Shenzhen Environmental Science and New Energy Technology Engineering Laboratory, Tsinghua-Berkeley Shenzhen Institute, Shenzhen 518055, P. R. China*
[d] *School of Electronic Science and Engineering, Nanjing University, Nanjing 210023, China*

† Electronic supplementary information (ESI) available: Table S1 presents a relative abundance of metabolites before and after reaction during formation of AgNPs; Tables S2 and S3 presents the process of optimization of reaction conditions, including pH, reaction temperature, reaction time and the ratio of $AgNO_3$ and leaf extracts. Fig. S1–S3 show trials to optimize the reaction conditions; Fig. S4 shows the stability of the synthesized AgNPs; Fig. S5 is a representative chromatogram (TIC) from GC-MS. See DOI: 10.1039/c8nj06291a

‡ H. Z. and Y. H. contributed equally to this manuscript, considered as co-first authors.

they speculated that reducing sugars are likely to be responsible for the reduction of Ag^+ to Ag. Some studies[14,18] showed that polysaccharides, proteins, flavonoids and terpenoids, which together promote the total reducing capacity of plant cells, could be involved in the biosynthesis of metal NPs and their stabilization. Kahrilas *et al.*[19] determined the metabolites in an orange peel extract and assumed that aldehyde-containing and other reducing compounds participated in the generation of AgNPs. Begum *et al.*[20] proposed that polyphenols or flavonoids present in tea leaves were responsible for the synthesis of AgNPs. This conclusion was reached since no AgNPs were observed in the leaf extract lacking polyphenols/flavonoids.

However, most of the proposed mechanisms were just reasonable hypotheses, lacking direct experimental evidence.[13] In order to elucidate the underlying mechanism, metabolites must be precisely quantified before and after the reaction. Metabolomics was originally used to study the metabolic response of organisms to their environment. By using gas chromatography-quadrupole time-of-flight mass spectrometry (GC-QTOF-MS) based metabolomics, we were able to identify and semi-quantify the relative level of hundreds of metabolites simultaneous in cucumber leaves and the cucumber root exudate.[21,22] We hypothesized that metabolomics can provide important screening information to identify and semi-quantitatively analyze the metabolites that are involved in the AgNP biosynthesis process.

Based on the metabolomics screening data, we propose to further obtain the key thermodynamic data by using isothermal titration calorimetry (ITC), which can directly measure the heat absorbed or released during the interaction to determine the changes in enthalpy ΔH, entropy ΔS and Gibbs free energy ΔG of the adsorption process, as well as the affinity binding constant K_d and the stoichiometry of the interaction reaction.[23] Combining these two novel approaches, the mechanism of AgNPs green synthesis would be revealed at the molecular level.

Cucumber leaves are agricultural by-products and have high levels of reducing metabolites.[24,25] In this study, the cucumber leaf extract was prepared and used as a reducing and stabilizing agent for AgNPs biosynthesis. After the AgNP synthesis conditions were optimized and AgNPs were synthesized, the physicochemical properties of the obtained NPs were characterized using UV-vis spectrophotometry, dynamic light scattering (DLS) and transmission electron spectroscopy (TEM) and single particle inductively coupled plasma mass spectrometry (sp-ICP-MS). In addition, GC-MS was employed to determine the content of metabolites before and after the reaction, by which, the role of specific reducing agents can be elucidated. The key thermodynamic data of the interaction between Ag^+ and cucumber leaf extracts were determined *via* the ITC measurement. Finally, the antioxidant capacity of the AgNPs was evaluated.

Materials and method

Preparation of cucumber leaf extracts

Cucumber seeds (Zhongnong No. 28 F1) were purchased from Hezhiyuan Seed Corporation (Shandong, China). Before use, the seeds were treated with 5% NaClO for 30 min. After complete rinsing, the seeds were germinated in quartz sand in the dark at 25 °C for 7 days. After germination, the plants were transferred into Hoagland nutrient solution and cultivated for 5 weeks to generate sufficient biomass. The nutrient solution was replaced once per week. The cucumber leaves were harvested when the cucumber plants were 5 weeks old. Fresh cucumber leaves were collected and washed with DI water and oven-dried at 105 °C for 30 min followed by 70 °C for 8 h. To prepare the leaf extract, 10 grams of the oven-dried leaves powder was added to 100 mL of DI water and the mixture was boiled at 100 °C for 15 min. After cooling down, the solution was centrifuged at 10 000 rpm for 10 min and the supernatant was collected and stored at 4 °C.

Chemicals

DI water was used for all the experiments. Silver nitrate ($AgNO_3$; Shanghai Reagent Company; ≥99.8%), ammonium hydroxide (NH_4OH; Aladdin Industrial Corporation (Shanghai, China); 25–28%); hydrochloric acid (HCl; 36–38%) and sodium hydroxide (NaOH; ≥96%) (Sinopharm Chemical Reagent Co., Ltd) (Shanghai, China), were used in this study without further purification.

All chemicals and solvents for GC-MS analysis were of analytical or HPLC grade. Water, methanol, pyridine, *n*-hexane, methoxylamine hydrochloride (97%) and BSTFA with 1% TMCS were purchased from CNW Technologies GmbH (Düsseldorf, Germany). Trichloromethane was purchased from Sinopharm Chemical Reagent Co., Ltd (Shanghai, China). L-2-Chlorophenylalanine was from Shanghai Hengchuang Bio-technology Co., Ltd (Shanghai, China).

Biosynthesis of silver NPs using cucumber leaf extracts

An initial screening trial using UV-vis was performed to optimize the AgNP synthesis conditions, including pH, reaction temperature, reaction time and the ratio of $AgNO_3$ and leaf extracts (Tables S2 and S3; Fig. S1 and S2, ESI†). The formation of AgNPs was confirmed by measuring the UV-vis spectra at 414 nm and color changes. UV-vis spectroscopic analyses of AgNPs were carried out as a function of the reaction time and temperature using a microplate reader (Synergy H4 Hybrid Reader, Biotek, America) at a resolution of 2 nm. According to the preliminary assays, $AgNO_3$ at a concentration of 10 mM, leaf extract and $AgNO_3$ at a volume ratio of 1 : 1, pH 10.0, reaction time of 4 h, and a reaction temperature of 80 °C were the optimal conditions to synthesize AgNPs (Fig. S3, ESI†).

Characterization of Ag nanoparticles

The newly synthesized NPs were characterized using DLS, TEM and sp-ICP-MS. The hydrodynamic size and zeta potential of the nanoparticles were measured using a zetasizer nano ZS (Malvern Instrument, USA). Morphological characteristics were performed using a transmission electron microscope (TEM) (JEM-200CX, JEOL, Japan).

sp-ICP-MS measurements

An Agilent 7900 ICP-MS (Santa Clara, CA, USA) was used to perform the sp-ICP-MS analysis to determine the particle size

Table 1 The optimized instrumental setting for the AgNP analysis in sp-ICP-MS

Parameter	Value
RF power	1550 W
Carrier gas	0.67 L min^{-1}
Make-up gas	0 L min^{-1}
Spray chamber temperature	2 °C
Nebulizer pump	0.1 rps
Sample depth	8.0 mm
Oxide ratio	1%
Integration time	100 μs
Acquisition time	90 s
Mass monitored	^{107}Ag

and concentration of the synthesized AgNPs. Analyses were performed in a time resolved analysis (TRA) mode using an integration time (dwell time) of 100 μs per point with no settling time between measurements. The instrumental settings used for the sp-ICP-MS analysis are summarized in Table 1, which were modified based on a previous study.[26] The sp-ICP-MS method setup, data collection and analysis were conducted *via* single nanoparticle application module of the Agilent ICP-MS MassHunter software (Version C.01.04 Build 544.3).

An AgNP standard (60 nm, Agilent, USA) was diluted to 100 ng L^{-1} Ag (99%) with DI water in metal-free polypropylene tubes, to evaluate the nebulization efficiency, which was used in the data conversion from a raw signal to the NP size. An Ag ionic standard of 1 μg L^{-1} was prepared with 1% HNO_3 and was used to determine the elemental response factor. The samples were diluted with DI water to ensure that AgNP concentrations were between 50 and 200 ng L^{-1}, and a sample inlet flow of 0.346 mL min^{-1} was used. The analyte mass fraction was set to 1 while the particle density was set to 10.5 g cm^{-3}. NP sample preparation and dilution were performed on the day of the analysis to avoid sample degradation and minimize transformation of the AgNPs after processing. Before dilution of the samples and again prior to their analysis, all solutions were placed in an ultrasonic bath for 10 min to ensure that the samples were fully homogenized.

Isothermal titration calorimetry measurements

A TA Instruments nano isothermal titration calorimeter (nITC) (TA Instruments-Waters LLC, DE, US) was used to measure the heat exchange between Ag^+ and the cucumber leaf extracts at 298 K to identify physicochemical interactions as well as determine the thermodynamic data and binding constants.[27]

An Ag^+ solution (1 mM), prepared in degassed DI water (pH 10), was loaded into the 100 μL injection syringe; and a solution of fructose (20 mM) was placed in the 1 mL nITC sample cell (the concentration of fructose was generally 10–20 times higher than the concentration of Ag^+ to obtain a strong heat exchange signal as well as to ensure that interaction equilibrium is reached. The difference in the concentration ratio would not change the output significantly[28]). The rotational speed of the stirrer was 250 min^{-1} to ensure proper mixing. Ag^+ was titrated into the sample cell as a sequence of 20 injections of 4.91 μL aliquots. The equilibrium time between the two injections was set at 800 s for the signal to return to the baseline.

Estimated binding parameters were obtained from the nITC data using the NanoAnalyze data analysis software (Version 3.60). Data fits were obtained using the independent set of multiple binding sites (MNIS) model,[29] for which the analytical solution for the total heat measured, Q (kJ) is determined by the formula:

$$Q = \frac{(1 + [M]nK_d + K_d[L_T]) - \left[(1 + [M]nK_d + K_d[L_T])^2 - 4[M]nK_d^2[L_T]\right]^{1/2}}{\frac{2K_d}{V\Delta H}} \quad (1)$$

where V is the volume of the calorimeter cell, ΔH is the enthalpy (kJ mol^{-1}), and K_d (M^{-1}) is the equilibrium binding constant. Free energy, ΔG (kJ mol^{-1}), was determined from the binding constant ($\Delta G = -RT\ln K$, where R is the gas constant and T is the absolute temperature in Kelvin) and entropy, ΔS (kJ mol^{-1}), from the second law of thermodynamics ($\Delta G = \Delta H - T\Delta S$). $[L_T]$ is the total ligand concentration and [M] is the macromolecular concentration, n is the molar ratio of interacting species. To consider the jth injection, the molar ratio can be calculated as:

$$n = \frac{[L_j]}{[M]} \quad (2)$$

with

$$L_j = L_{j-1} + V_j \cdot [L]_m \quad (3)$$

$$M = [M]_m \cdot V \quad (4)$$

where V_j is the volume of each titration, while $[L]_m$ and $[M]_m$ are the molar concentrations of the ligand and macromolecules. In the current study, since Ag^+ was titrated into the fructose solution, we considered Ag^+ as the ligand (L), and fructose as macromolecules (M).

Metabolomics to determine molecules responsible for reducing and stabilizing

Metabolites in leaf extracts before and after the reaction were analyzed using GC-MS to determine the metabolites playing key roles in the synthesis of AgNPs.

Sample preparation. 400 μL of the extract was transferred to a 1.5 mL Eppendorf tube, followed by addition of 200 μL of chloroform and 20 μL of 2-chloro-l-phenylalanine (0.3 mg mL^{-1}) dissolved in methanol as an internal standard. The mixtures were vortexed for 1 min and ultrasonicated for 30 min at the ambient temperature. The mixtures were centrifuged at 12 000 rpm for 10 min at 4 °C. An aliquot of 200 μL supernatant was transferred into a glass sampling vial for vacuum-drying at room temperature. Then 80 μL of 15 mg mL^{-1} methoxylamine hydrochloride in

pyridine was subsequently added. The resulting mixture was vortexed vigorously for 2 min and incubated at 37 °C for 90 min. Then, 80 μL of *N*,*O*-bis(trimethylsilyl)trifluoroacetamide (BSTFA) (with 1% trimethylchlorosilane) and 20 μL *n*-hexane were added into the mixture, which was vortexed vigorously for 2 min and then derivatized at 70 °C for 60 min. The samples were placed at room temperature for 30 min before GC-MS analysis.

GC-MS analysis. The derivatized samples were analyzed in an Agilent 7890B gas chromatography system coupled to an Agilent 5977A mass selective detector (Agilent Technologies Inc., CA, USA). The column was a DB-5MS fused-silica capillary column (30 m × 0.25 mm × 0.25 μm; Agilent Technologies, Santa Clara, CA). Helium (>99.999%) was used as the carrier gas at a constant flow rate of 1.0 mL min^{-1} through the column. The initial oven temperature was 60 °C, ramped to 125 °C at a rate of 8 °C min^{-1}, to 210 °C at a rate of 4 °C min^{-1}, to 270 °C at a rate of 5 °C min^{-1}, to 305 °C at a rate of 10 °C min^{-1} and finally held at 305 °C for 3 min. The injection volume was 1 μL, with the injector temperature of 260 °C and in a splitless mode. The temperature of the MS quadrupole and ion source (electron impact) was set to 150 and 230 °C, respectively. The collision energy was 70 eV. Mass data was acquired in a full-scan mode (*m*/*z* 50–500), and the solvent delay time was set to 5 min. The QCs were injected at regular intervals (every 10 samples) throughout the analytical run to provide a set of data from which repeatability can be assessed. A representative chromatogram (TIC) from GC-MS is shown in Fig. S5 (ESI†).

Determination of total reducing sugars

Total reducing sugars were determined based on the 3,5-dinitrosalicylic acid (DNS) method.[30] The liquid before and after the reaction was centrifuged at 10 000 rpm for 30 min, then 1 mL of the supernatant was mixed with 2 mL of DNS reagent and boiled for 5 min. After cooling the sample down to room temperature, the absorbance was determined at 540 nm using a UV-vis spectrometer (UV-1800, Shimadzu, Japan). The final result was expressed as mg glucose equivalent per mL liquid.

Determination of total phenolic compounds

Total phenolic compounds were determined based on the method by Singleton *et al.*[31] Briefly, 50 μL of the supernatant was mixed with 450 μL of DI water, then 250 μL of 2 M Folin-Ciocalteu reagent and 1.25 mL of 20 g L^{-1} Na_2CO_3 were added. The absorbance was measured at 735 nm using a UV-vis spectrometer (UV-1800, Shimadzu, Japan). The final concentration was expressed as μg gallic acid equivalent per mL liquid.

Results and discussion

Optimal conditions for the green synthesis of AgNPs

Preliminary experiments were conducted to optimize synthesis conditions, including the pH, reaction time and temperature. Totally 54 trials were completed with various combinations of pH (4.02, 5.86 and 10.01), reaction time (0.5, 1, 2 and 4 h), reaction temperature (25, 50 and 80 °C), and $AgNO_3$/leaf extract ratios (1 : 4, 1 : 1, 2 : 1 and 4 : 1) (ESI,† Fig. S1 and S2). The approached optimized conditions for AgNP formation: reaction time = 4 h; reaction temperature = 80 °C; pH = 10.01; $AgNO_3$/leaf extract ratio = 1 : 1 (Fig. S3, ESI†). We found that pH and temperature of the reaction system were the most important factors for the biosynthesis of AgNPs using cucumber leaf extract. Yun *et al.*[32] hypothesized that a higher pH generates a large number of functional groups, which facilitates a higher number of Ag(I) to bind and subsequently form smaller NPs. Upon mixing of 1.25 mL of 10 mM $AgNO_3$ with 1.25 mL of cucumber leaf extract at 80 °C for 4 h and pH adjusted to 10.0 using 200 μL ammonium hydroxide, the color changed from yellow to brownish-yellow, which indicated the formation of AgNPs (Fig. 1A). The color change was caused by the surface plasmon resonance (SPR) of AgNPs in the visible region.[33,34] This plasmon resonance is an intrinsic property of AgNPs and arises from the coupling between the electron cloud on the surface of AgNPs with the incident electromagnetic radiation. Therefore, the color change is a clear indicator of AgNP formation. The formation of AgNPs in the reaction solution was further confirmed by UV-visible spectroscopy. A single sharp intense peak at 414 nm (Fig. 1A) was observed, suggesting the existence of AgNPs, since the characteristic peak of AgNPs is between 380 to 420 nm depending on the size of the AgNPs.[35,36]

AgNP characterization

The particle size distribution of the synthesized AgNPs in suspension was determined by TEM and DLS. A typical TEM image reveals that the particles are roughly spherical in shape with sizes in the range of 5–25 nm (average size 13.7 nm) (Fig. 1B and C). The average hydrodynamic diameter of the AgNPs in DI water is 75.7 ± 2.8 nm, with a zeta potential of −19.82 ± 0.11 mV. To investigate the stability of AgNPs, hydrodynamic size and zeta potential were monitored for 0, 7, 14 and 36 days. Results showed that the hydrodynamic size of AgNPs was stable for 36 days, indicating high stability of the synthesized NPs (Fig. S4, ESI†).

Transformation process from Ag ions to AgNPs

sp-ICP-MS was employed to obtain more detailed information regarding the particle number, mass concentration, particle size and elemental composition of the synthesized AgNPs, which was conducted in a time-dependent setup (Fig. 2) investigating the nucleation and crystal growth. After heating at 80 °C with the cucumber leaf extract for 30 min, AgNPs with a most frequent size of 40.67 ± 1.15 nm were detected (Table 2), indicating fast nucleation of AgNPs. Noticeably, there was a small portion of AgNPs with size larger than 100 nm as shown in the blue bar in Fig. 2A. With increasing reaction time, the size of the AgNPs continued to increase; the largest mean size (76.42 ± 1.33 nm) was achieved after 4 h reaction (Table 2). However, even after 4 h reaction, the most frequent size was determined to be almost unchanged (42.00 ± 2.00 nm) compared to that (40.67 ± 1.15 nm) at 30 min of reaction time. It suggested that most of the newly synthesized AgNPs show a relatively narrow size distribution,

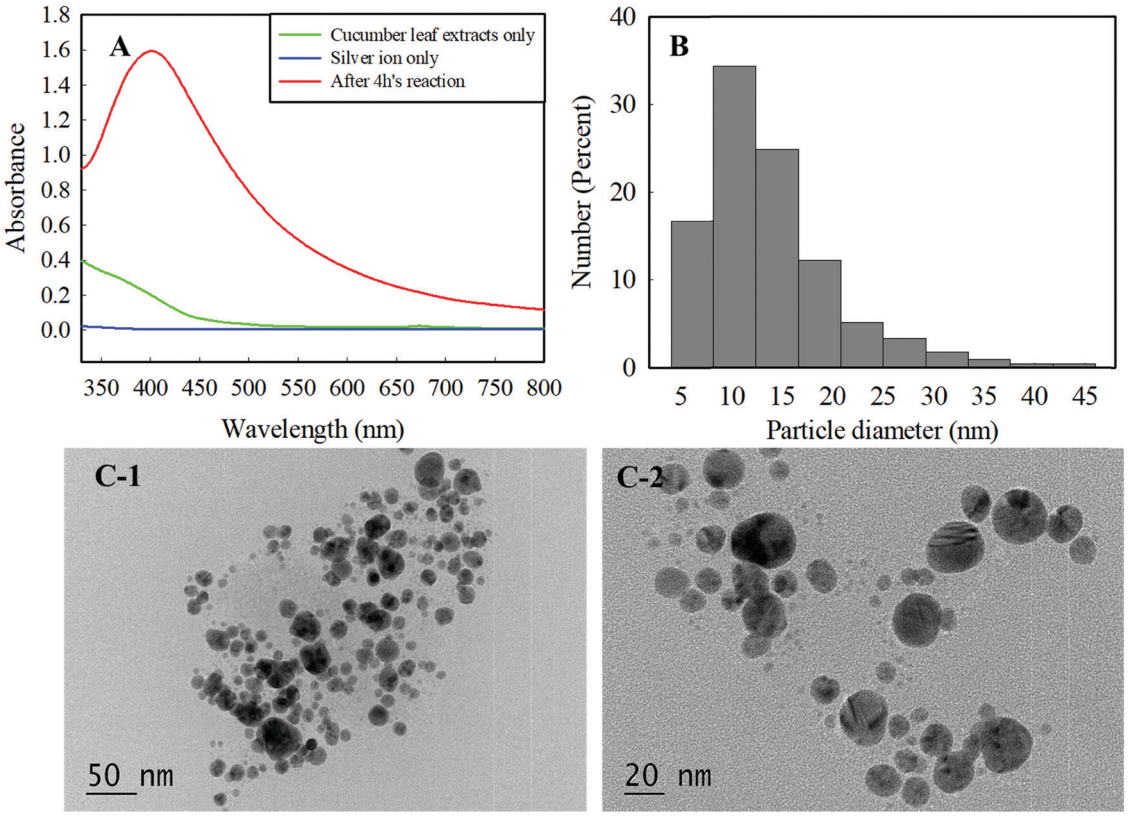

Fig. 1 (A) UV-vis spectrum of AgNPs synthesized by reduction of aqueous Ag ion solution with the cucumber leaf extract (pH 10, reaction temperature 80 °C, reaction time 4 h, $AgNO_3$: leaf extract = 1 : 1). (B) TEM size distribution of AgNPs. (C) Representative TEM images of the AgNPs prepared using cucumber leaf extracts with a scale bar of (C-1) 1 μm (20 000× magnification); and (C-2) 100 nm (37 000× magnification).

which would not be affected by the reaction time. The mean size of AgNPs increased from 58.06 ± 0.29 nm to 76.42 ± 1.33 nm as the reaction proceeded (Fig. 2), which was consistent with the DLS measurements. As the reaction time has been extended, the portion of larger size (>100 nm) AgNPs significantly increased, shown as the blue bars in Fig. 2, which indicated time-dependent AgNP crystal growth. The concentration of synthesized AgNPs increased from 51.76 to 219.32 mg L^{-1}, meanwhile, the concentration of Ag ions decreased from 215.80 to 46.33 mg L^{-1} at the end of the 4 h reaction time (Fig. 3), which suggested that Ag^+ ions were sequentially transformed to AgNPs during the green synthesis process. This demonstrates that the current green synthesis is a rapid (>0.5–4 h) and efficient way to prepare AgNPs with the yield rate of 49.19 ± 0.66%.

Metabolites responsible for the Ag nanoparticle formation

Cucumber plants contain various metabolites including sugars, amino acids, phenolic compounds, fatty acids and other secondary metabolites. A variety of metabolites have the ability to reduce Ag^+ to Ag(0), such as sugars, ascorbic acid and phenolic compounds. Table 3 presents the relative concentration of metabolites before and after the reaction, from the GC-MS based metabolomics. We considered that metabolites with a concentration decrease higher than 1.2 fold were responsible for the reactions, and can either act as reducing or stabilizing agents. There were in total 40 compounds whose relative concentrations were significantly ($p < 0.05$) decreased (Table 3). Most of the significantly changed metabolites were sugars and organic acids, indicating that sugars and organic acids played an important role in reducing Ag ions to AgNP.

Sugars and sugar alcohols. It is interesting to note that a number of sugar and sugar derivatives, such as cellobiose, D-glucoheptose, ribulose-5-phosphate, melibiose, 2-deoxy-D-glucose, tagatose, fructose, ribose and 3,6-anhydro-D-galactose (Fig. 4) were significantly ($p < 0.05$) decreased after the reaction. Those sugar and sugar derivatives were possibly involved in the formation of AgNPs and likely function as a reducing agent. Shankar *et al.* hypothesized that reducing sugars in the Neem leaf extract could be responsible for the reduction of metal ions to the corresponding metal NPs.[37] However, this hypothesis was not proven valid for the Neem leaf extract. Not surprisingly, non-reducing sugar like sucrose, were unchanged in the cucumber leaf extracts after the reaction. In addition, sugar alcohols like mannitol, threitol and galactinol (Table S1, ESI†) were unchanged, indicating that they did not participate in the reaction. We further analyzed total reducing sugar before and after the reaction with the cucumber leaf extract. We hypothesized that total reducing sugars should decrease during the formation of AgNPs. Surprisingly, total reducing sugars content increased by 227% after the reaction, which could be due to the fact that polysaccharides were

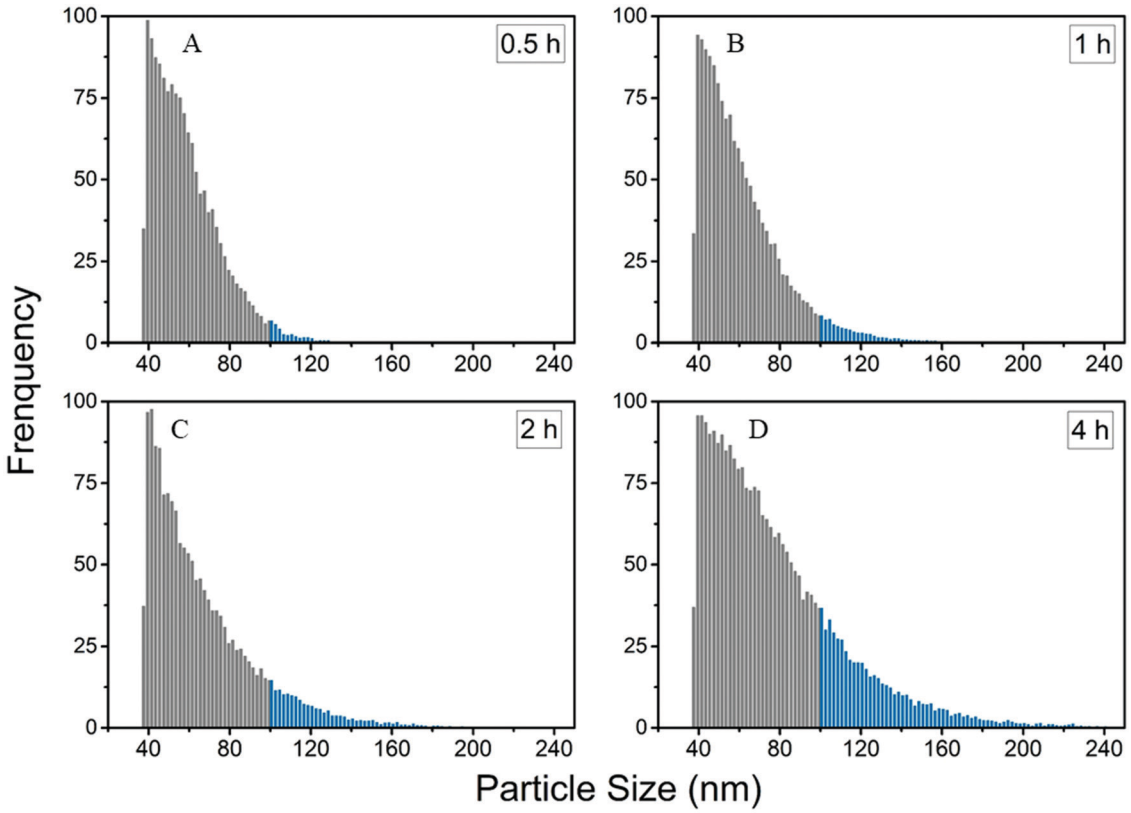

Fig. 2 Size distribution measured *via* sp-ICP-MS of AgNPs synthesized by cucumber leaf extract at 80 °C after (A) 30 min; (B) 1 h; (C) 2 h and (D) 4 h. The blue bars represent the frequency of AgNPs with a size larger than 100 nm.

Table 2 Median, mean and most frequent size of AgNPs synthesized with cucumber leaf extract at different reaction time, as measured by sp-ICP-MS. (The values of average and standard deviation were calculated from triplicate measurements)

Reaction time (h)	Median size (nm)		Mean size (nm)		Most frequent size (nm)	
	Avg	Std	Avg	Std	Avg	Std
0.5	54.63	0.20	58.06	0.29	40.67	1.15
1	55.32	0.42	60.31	0.49	40.67	1.15
2	58.10	0.18	65.45	0.26	41.33	1.15
4	68.52	1.26	76.42	1.33	42.00	2.00

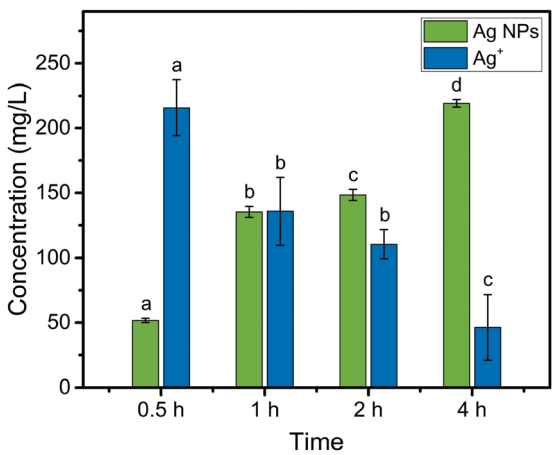

Fig. 3 AgNP and Ag ion concentration measured *via* sp-ICP-MS at different synthesis times (30 min, 1 h, 2 h and 4 h). The AgNPs were synthesized by adding 1.25 mL of the leaf extract to 1.25 mL of $AgNO_3$ and heated at 80 °C at pH 10. Data are the mean of three replicates, and error bars represent ± standard error. Different letters stand for statistical differences at $p \leq 0.05$ (Tukey's HSD multiple comparisons at $p \leq 0.05$).

degraded into reducing single sugars, thus maintaining a high level of total reducing sugars.

To further investigate the role of the sugars as the reducing agent in AgNPs green synthesis process, ITC was applied to identify and detect the physicochemical interactions between cucumber leaf extracts and Ag^+. Based on the metabolomics screening results and our hypotheses, we chose fructose as a case study to discuss that sugars were acting as reducing agents from the thermodynamic perspective.[27] The heat exchange as a function of time as Ag^+ was titrated into the fructose solution was shown in the real-time thermogram (Fig. 5A). Each injection of Ag^+ results in heat change due to the binding between Ag^+ and fructose within the sample cell, causing a change in the heat flow, shown as peaks in the thermogram (Fig. 5A). The interaction between Ag^+ and fructose was exothermic, and the peak amplitudes and area gradually decreased as more Ag^+ was added since the number of available binding sites

Table 3 Relative abundance of metabolites before and after reaction during the formation of AgNPs. (The relative abundance values were reported as the "average ± standard deviation" of the three replicates)

Metabolites	Classification	Relative abundance		Fold
		Before	After	
2-Amino-2-norbornanecarboxylic acid	Organic acid	1.47 ± 0.01	0.00 ± 0.00	
Cellobiose	Sugar	4.94 ± 0.52	0.00 ± 0.00	
Biuret		2 ± 0.02	0.06 ± 0.09	31.5
D-Glucoheptose	Sugar	6.85 ± 0.54	0.72 ± 0.04	9.6
Pyruvic acid	Organic acid	49.22 ± 2.33	6.63 ± 2.07	7.4
Alpha-ketoglutaric acid	Organic acid	4.66 ± 0.66	0.81 ± 0.26	5.8
2-Amino-2-methylpropane-1,3-diol		7.35 ± 0.04	1.56 ± 0.39	4.7
Glucoheptonic acid	Organic acid	205.29 ± 13.7	77.19 ± 20.28	2.7
N-Acetyl-L-glutamic acid	Organic acid	35.92 ± 3.94	15.7 ± 2.15	2.3
5-Aminoimidazole-4-carboxamide		0.96 ± 0.03	0.42 ± 0.01	2.3
1-Methylhydantoin		71.86 ± 2.69	33.39 ± 2.39	2.2
Cumic acid	Organic acid	3.48 ± 0.07	1.67 ± 0.03	2.1
L-Allothreonine		36.99 ± 0.2	18.44 ± 6.49	2.01
N-Acetyl-5-hydroxytryptamine		2.14 ± 0.08	1.06 ± 0.04	2.0
Melibiose	Sugar	9.9 ± 0.44	5.27 ± 0.65	1.9
2-Deoxy-D-glucose	Sugar	7.18 ± 0.45	3.85 ± 0.58	1.9
Hesperitin		0.11 ± 0.02	0.06 ± 0.01	1.88
Tagatose	Sugar	203.88 ± 8.39	111.95 ± 15.98	1.8
Dibenzofuran		13.63 ± 0.94	7.83 ± 0.34	1.7
Farnesol	Alcohol	0.28 ± 0.01	0.17 ± 0.00	1.7
Benzoylformic acid	Organic acid	0.38 ± 0.01	0.23 ± 0.04	1.6
Squalene	Alkene	0.37 ± 0.01	0.23 ± 0.01	1.6
Methyl octanoate	Ester	4.37 ± 0.12	2.71 ± 0.03	1.6
Indole-3-acetamide		0.77 ± 0.09	0.49 ± 0.03	1.6
Alpha-ketoisocaproic acid	Organic acid	4.46 ± 0.25	2.82 ± 0.28	1.6
N,*N*-Dimethylarginine		5.65 ± 0.33	3.58 ± 0.36	1.6
P-Benzoquinone		25.69 ± 0.85	16.34 ± 0.51	1.6
Fructose	Sugar	291.27 ± 12.51	186.66 ± 27.54	1.6
2-Keto-isovaleric acid	Organic acid	1.68 ± 0.07	1.08 ± 0.16	1.6
Stearic acid	Fatty acid	0.85 ± 0.14	0.57 ± 0.05	1.51
Nicotinoylglycine		1.81 ± 0.07	1.17 ± 0.03	1.5
4-Hydroxymethyl-3-methoxyphenoxyacetic acid	Organic acid	0.52 ± 0.01	0.34 ± 0.03	1.5
2-Aminoethanethiol		26.57 ± 0.54	17.83 ± 0.57	1.5
Palmitic acid	Fatty acid	1.11 ± 0.14	0.77 ± 0.02	1.44
N-Alpha-acetyl-L-ornithine	Organic acid	17.97 ± 1.22	12.66 ± 0.94	1.4
Pelargonic acid	Organic acid	0.27 ± 0.01	0.19 ± 0.01	1.4
Aminomalonic acid	Organic acid	0.30 ± 0.00	0.23 ± 0.01	1.4
Ribose	Sugar	35.58 ± 1.17	26.33 ± 2.83	1.4
3-Methylamino-1,2-propanediol	Alcohol	2.22 ± 0.07	1.68 ± 0.15	1.3
3,6-Anhydro-D-galactose	Sugar	24.64 ± 0.22	20.07 ± 0.50	1.2

decreased. Eventually, only a low heat exchange was observed for the last several injections corresponding to dilution, once binding sites were saturated.

The energy exchange as a function of the ratio between Ag^+ and fructose was presented in Fig. 5B. The independent set of multiple binding sites (MNIS) model (eqn (1))[29] was applied to process the data, and the fitted and calculated thermodynamic parameters suggested that the interactions between Ag^+ and fructose were thermodynamically identical. It's an energetically favored spontaneous process with $\Delta G = -30.45$ kJ mol^{-1}, and the interactions were enthalpically driven with a negative ΔH value (-109.8 kJ mol^{-1}). The stoichiometric values ($n = 0.001$) was much smaller than unity, indicating that due to the relatively low reducing power, more fructose molecules were involved in the reduction process.

Thus, the ITC results demonstrate the important role of the sugars from cucumber leaf extracts in the green synthesis process of AgNPs.

Phenolic compounds. Phenolic compounds possess hydroxyl and carboxyl groups, and may inactivate metal ions by chelating and additionally suppressing the superoxide-driven Fenton reaction, which is believed to be the most important source of reactive oxygen species (ROS). Therefore, plants with high content of phenolic compounds (*e.g.* Pinus species) are some of the best candidates for nanoparticle synthesis.[3] It has been reported that polyphenols can be adsorbed on the surface of metallic nanoparticles through the interaction with their carbonyl groups.[14] The mechanism of converting ketone groups into carboxylic acid in flavonoids was proposed to play an important role during the conversion of Ag^+ to Ag. Unexpectedly, all of the detected phenolic compounds, including 1,2,4-benzenetriol, caffeic acid, ferulic acid and hydrocinnamic acid, were unchanged during the reaction (Table S1, ESI†), which indicated that these compounds did not participate in the reaction. We further determined total phenolic compounds in the system before and after the reaction, and we found no changes in the total phenolic compound content.

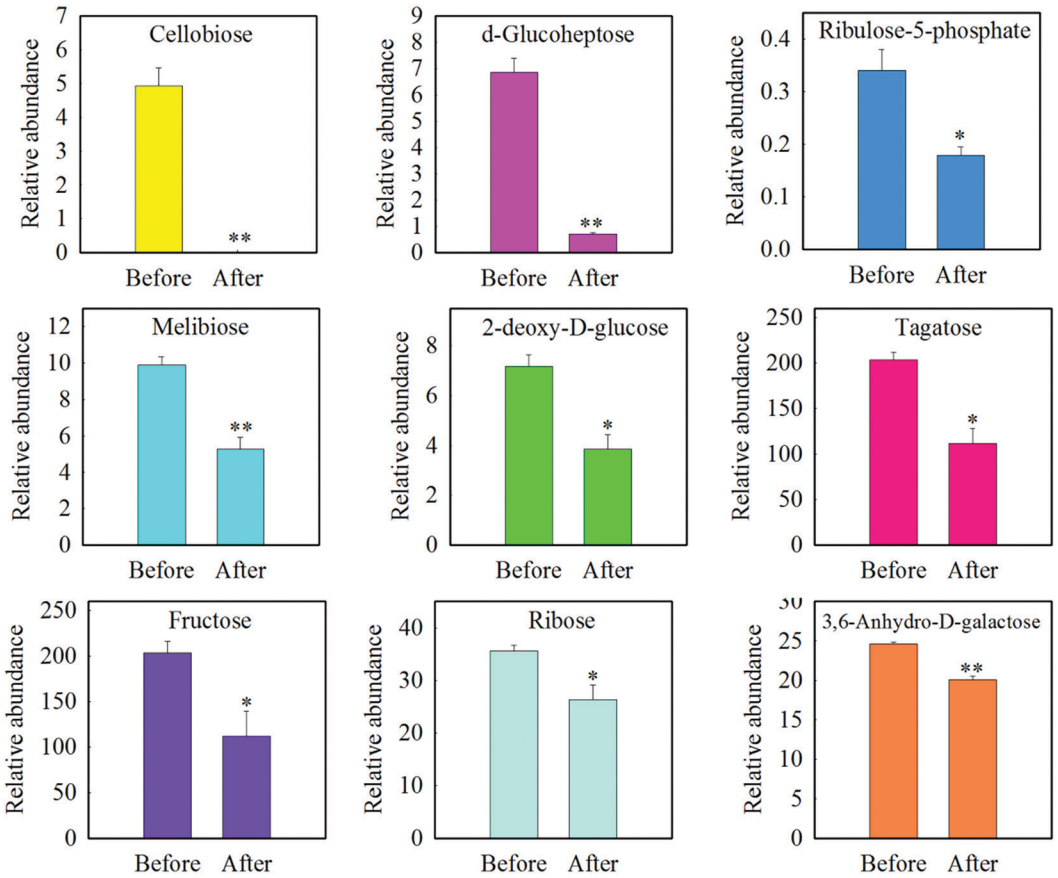

Fig. 4 The relative abundance of significantly changed sugars determined by GC-MS in solution before and after the reaction. The AgNPs were synthesized by adding 1.25 mL of the leaf extract to 1.25 mL of $AgNO_3$ and heated at 80 °C at pH 10.

This further confirmed that phenolic compounds did not play a role in the process of reducing Ag ions to AgNPs.

Amino acids. The levels of most of the amino acids, including alanine, asparagine, lysine, valine, isoleucine, proline, serine, threonine, beta-alanine, tyrosine and tryptophan, were unchanged after reaction in this study (Table S1, ESI†). This indicates that amino acids did not play an important role in the reduction of Ag ion to AgNPs. Gruen[38] reported that arginine, cysteine, lysine and methionine, out of twenty amino acids, were able to interact with Ag^+.

Organic acids. Pyruvic acid, generated from the redox reactions in the glycolytic pathway, was decreased 7-fold after the reaction (Table 3), indicating it participated in the synthesis, possibly acting as a reducing agent.[14] In addition to pyruvic acid, 2-amino-2-norbornanecarboxylic acid, alpha-ketoglutaric acid, glucoheptonic acid, *N*-acetyl-L-glutamic acid and cumic acid decreased approximately 2- and 6-fold, respectively, which indicates these two carbohydrate acids likely participated in the formation of AgNPs.

Citric acid and oxalic acid have been hypothesized to be involved in the reduction of Ag^+ to AgNPs.[39,40] Prathna *et al.*[40] predicted that citric acid could act as both the principal reducing agent and stabilizing agent during the AgNP synthesis. In our study, neither oxalic nor citric acid changed their concentration, indicating they were not involved in the reduction and that citric acid or citrate would not be the principal stabilizing agent in a more complex mixture of organic compounds such as cucumber leaf extract (Table 3).

Fatty acid. Interestingly, two saturated fatty acids stearic acid and palmitic acid exhibited decreases in concentration by approximately 1.5-fold after reaction (Table 3). Since it is unlikely that these fatty acids would have the capacity to reduce Ag^+ to Ag, we hypothesize that they act as capping agents on the surface of AgNPs. A previous study indicated that fatty acids can act as stabilizing agents in the synthesis of silver nanoparticles.[41–43] Nagasawa *et al.*, showed that coating silver nanoparticles with fatty acids (myristic, stearic and oleic acid) stabilized the nanoparticles, preventing their aggregation.[41]

In summary, through GC-MS based metabolomics a number of metabolites were found to be responsible for reduction of Ag ions to AgNPs. But it has to be noted that higher molecular weight compounds such as proteins may also play an important role in the formation of AgNPs. Previous studies reported that proteins can bind to Au nanoparticles through their free amine groups or carboxylate ions.[14] Bali *et al.* proposed that protein not only act as reducing agent, but also can act as stabilizing agents.[44] Apart from proteins, even polysaccharide may act as a reducing agent in nanoparticle biosynthesis, which needs to be explored in future study.

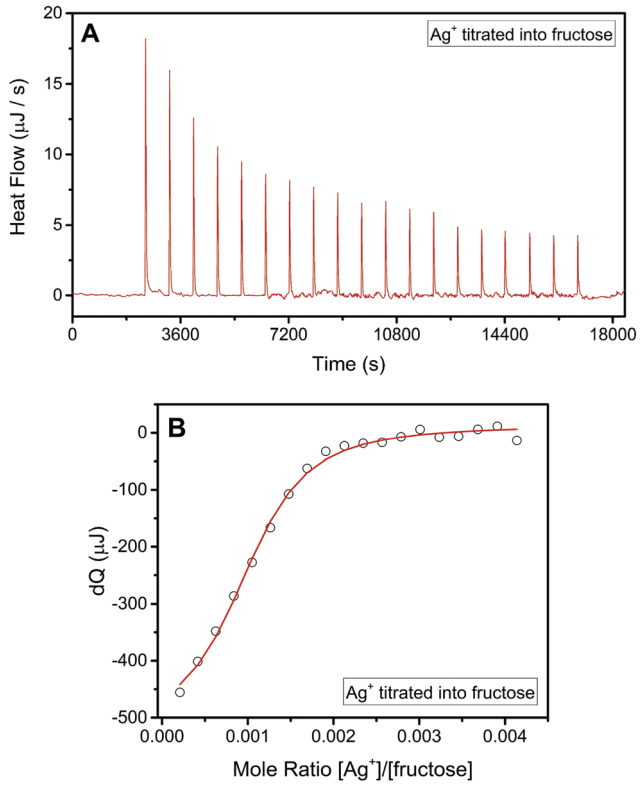

Fig. 5 (A) Thermograms for Ag^+ titration into fructose solutions at 298 K. Heat flow reflects the differential signal, with positive peaks indicating an exothermic process; (B) integrated heat data as a function of molar ratio of Ag^+ to fructose, fitted with the MNIS model. Symbols represent experimental data, and red lines represent the model prediction.

Conclusion

A simple one-pot green synthesis method using cucumber leaf extract to prepare AgNPs was developed. The formation kinetics of AgNPs was investigated *via* sp-ICP-MS, suggesting a fast generation process (less than 30 min). The synthesized AgNPs were stable, and no agglomerations were found in the 36-day period. GC-MS based metabolomics screened out the responsible metabolites in the green synthesis process. Specific reducing sugars (*e.g.*, cellobiose, fructose, ribose, *etc.*) and some organic acids were remarkably decreased during the green synthesis process, indicating the consumption of metabolites in the AgNP formation. The metabolomics results provided very valuable information with regards to the metabolites responsible for reducing Ag^+ and stabilizing the AgNPs. This is the first report that determines the key metabolites in a green synthesis method for AgNPs. The significant role of sugars in the biosynthesis of AgNPs was further thermodynamically identical and determined *via* ITC measurement. A thorough understanding of the underlying mechanisms involved in the synthesis process will enable this approach to be economically competitive with conventional methods.

Conflicts of interest

There are no conflicts of interest to declare.

Acknowledgements

This work was supported by the National Key Research and Development Program of China under 2016YFD0800207. We also acknowledge the National Natural Science Foundation of China under 21876081. Any opinions, finding, and conclusions or recommendations expressed in this material are those of authors and do not necessarily reflect the views of National Science Foundation of China. Arturo Keller thanks Agilent Technologies for the Agilent Thought Leadership award, which partially supported this work. Part of this work was supported by the National Science Foundation (NSF) and the U.S. Environmental Protection Agency (EPA) under NSF-EF0830117. The MRL Central Facilities supported by the MRSEC Program of the National Science Foundation under awards NO. DMR 1121053; a member of the NSF-funded Materials Research Facilities Network (www.mrfn.org). We thank the MRL Central Facilities for the use of their ITC.

References

1 P. P. Gan and S. F. Y. Li, *Rev. Environ. Sci. Bio/Technol.*, 2012, **11**, 169–206.
2 J. R. Peralta-Videa, Y. Huang, J. G. Parsons, L. Zhao, L. Lopez-Moreno, J. A. Hernandez-Viezcas and J. L. Gardea-Torresdey, *Nanotechnol. Environ. Eng.*, 2016, **1**, 1–29.
3 S. Iravani, *Green Chem.*, 2011, **13**, 2638–2650.
4 J. R. Peralta-Videa, Y. Huang, J. G. Parsons, L. Zhao, L. Lopez-Moreno, J. A. Hernandez-Viezcas and J. L. Gardea-Torresdey, *Nanotechnol. Environ. Eng.*, 2016, **1**, 4.
5 S. Iravani, *Green Chem.*, 2011, **13**, 2638–2650.
6 S. S. Momeni, M. Nasrollahzadeh and A. Rustaiyan, *J. Colloid Interface Sci.*, 2017, **499**, 93–101.
7 M. Maham, M. Nasrollahzadeh, S. M. Sajadi and M. Nekoei, *J. Colloid Interface Sci.*, 2017, **497**, 33–42.
8 S. Ahmed, Annu, S. Ikram and S. Yudha S, *J. Photochem. Photobiol., B*, 2016, **161**, 141–153.
9 Annu, A. Ali and S. Ahmed, in *Handbook of Ecomaterials*, ed. L. M. T. Martínez, O. V. Kharissova and B. I. Kharisov, Springer International Publishing, Cham, 2018, pp. 1–45.
10 S. Ahmed, Annu, I. Zafeer and S. Ikram, *J. Bionanosci.*, 2016, **10**, 47–53.
11 Annu, S. Ahmed, G. Kaur, P. Sharma, S. Singh and S. Ikram, *Toxicol. Res.*, 2018, **7**, 923–930.
12 Annu, S. Ahmed, G. Kaur, P. Sharma, S. Singh and S. Ikram, *J. Appl. Biomed.*, 2018, **16**, 221–231.
13 M. S. Akhtar, J. Panwar and Y.-S. Yun, *ACS Sustainable Chem. Eng.*, 2013, **1**, 591–602.
14 P. P. Gan and S. F. Y. Li, *Rev. Environ. Sci. Bio/Technol.*, 2012, **11**, 169–206.
15 R. Mohammadinejad, S. Karimi, S. Iravani and R. S. Varma, *Green Chem.*, 2016, **18**, 20–52.
16 D. Hebbalalu, J. Lalley, M. N. Nadagouda and R. S. Varma, *ACS Sustainable Chem. Eng.*, 2013, **1**, 703–712.
17 R. G. Haverkamp and A. T. Marshall, *J. Nanopart. Res.*, 2009, **11**, 1453–1463.

18 L. Marchiol, A. Mattiello, F. Poščić, C. Giordano and R. Musetti, *Nanoscale Res. Lett.*, 2014, **9**, 101.
19 G. A. Kahrilas, L. M. Wally, S. J. Fredrick, M. Hiskey, A. L. Prieto and J. E. Owens, *ACS Sustainable Chem. Eng.*, 2014, **2**, 367–376.
20 N. A. Begum, S. Mondal, S. Basu, R. A. Laskar and D. Mandal, *Biogenic synthesis of Au and Ag nanoparticles using Aqueous solutions of Black Tea leaf extracts*, 2009.
21 L. Zhao, Y. Huang, J. Hu, H. Zhou, A. S. Adeleye and A. A. Keller, *Environ. Sci. Technol.*, 2016, **50**, 2000–2010.
22 L. Zhao, Y. Huang, H. Zhou, A. S. Adeleye, H. Wang, C. Ortiz, S. Mazer and A. A. Keller, *Environ. Sci.: Nano*, 2016, **3**, 1114–1123.
23 Y. Huang and A. A. Keller, *Environ. Sci.: Nano*, 2016, **3**, 1206–1214.
24 L. Zhao, Y. Huang and A. A. Keller, *J. Agric. Food Chem.*, 2018, **66**, 6628–6636.
25 L. Zhao, Y. Huang and A. A. Keller, *J. Agric. Food Chem.*, 2017, 6628–6636.
26 A. A. Keller, Y. Huang and J. Nelson, *J. Nanopart. Res.*, 2018, **20**, 101.
27 Y. Huang, L. Zhao and A. A. Keller, *Environ. Sci. Technol.*, 2017, **51**, 9774–9783.
28 W. B. Turnbull and A. H. Daranas, *J. Am. Chem. Soc.*, 2003, **125**, 14859–14866.
29 E. Freire, O. L. Mayorga and M. Straume, *Anal. Chem.*, 1990, **62**, 950A–959A.
30 M. Ma, P. Wang, R. Yang and Z. Gu, *Food Chem.*, 2018, **250**, 259–267.
31 V. L. Singleton and J. A. Rossi, *Am. J. Enol. Vitic.*, 1965, **16**, 144–158.
32 M. Sathishkumar, K. Sneha, S. W. Won, C. W. Cho, S. Kim and Y. S. Yun, *Colloids Surf., B*, 2009, **73**, 332–338.
33 E. C. Njagi, H. Huang, L. Stafford, H. Genuino, H. M. Galindo, J. B. Collins, G. E. Hoag and S. L. Suib, *Langmuir*, 2011, **27**, 264–271.
34 J. Xie, J. Y. Lee, D. I. C. Wang and Y. P. Ting, *ACS Nano*, 2007, **1**, 429–439.
35 N. Aihara, K. Torigoe and K. Esumi, *Langmuir*, 1998, **14**, 4945–4949.
36 S. Alipilakkotte and L. Sreejith, *Mater. Lett.*, 2018, **217**, 33–38.
37 S. S. Shankar, A. Rai, A. Ahmad and M. Sastry, *J. Colloid Interface Sci.*, 2004, **275**, 496–502.
38 L. Clem Gruen, *Biochim. Biophys. Acta, Protein Struct.*, 1975, **386**, 270–274.
39 A. D. Dwivedi and K. Gopal, *Colloids Surf., A*, 2010, **369**, 27–33.
40 T. C. Prathna, N. Chandrasekaran, A. M. Raichur and A. Mukherjee, *Colloids Surf., B*, 2011, **82**, 152–159.
41 H. Nagasawa, M. Maruyama, T. Komatsu, S. Isoda and T. Kobayashi, *Phys. Status Solidi A*, 2002, **191**, 67–76.
42 N. Yang and K. Aoki, *J. Phys. Chem. B*, 2005, **109**, 23911–23917.
43 S. S. Lee, W. Song, M. Cho, H. L. Puppala, P. Nguyen, H. Zhu, L. Segatori and V. L. Colvin, *ACS Nano*, 2013, **7**, 9693–9703.
44 R. Bali and A. T. Harris, *Ind. Eng. Chem. Res.*, 2010, **49**, 12762–12772.